LOOKING INTO THE FUNCTIONAL ARCHITECTURE OF THE BRAIN WITH DIFFUSION MRI

Denis Le Bihan

Water diffusion magnetic resonance imaging (dMRI) allows tissue structure to be probed and imaged on a microscopic scale, providing unique clues to the fine architecture of neural tissues and to changes associated with various physiological and pathological states, such as acute brain ischaemia. Because diffusion is anisotropic in brain white matter, reflecting its organization in bundles of fibres running in parallel, dMRI can also be used to map the orientation in space of the white matter tracks in the brain, opening a new window on brain connectivity and brain maturation studies. This article provides an introduction to the key physical concepts that underlie dMRI, and reviews its potential applications in the neurosciences and associated clinical fields.

The ability to visualize anatomical connections between different parts of the brain, non-invasively and on an individual (rather than a statistical) basis, has opened a new era in the field of functional neuroimaging. This important breakthrough for neuroscience and related clinical fields has developed over the past ten years through the advance of diffusion magnetic resonance imaging (dMRI). The concept of dMRI is to produce MRI-based quantitative maps of microscopic, natural displacements of water molecules that occur in brain tissues as part of the physical diffusion process. Water molecules are used as a probe that can reveal microscopic details about the architecture of both normal and diseased tissue. The aim of this article is to introduce the main potential applications of dMRI in the neurosciences and associated clinical domains, such as neurology, neurosurgery and even psychiatry. A basic description of the diffusion process and the approaches used to measure and image diffusion with MRI is provided, as well as a review of our current understanding of the water diffusion process in the brain. For futher details on specific aspects of dMRI, I refer the reader to several extensive, detailed reviews that have been published recently.

The concept of molecular diffusion

Molecular diffusion refers to the random translational motion of molecules (also called Brownian motion) that results from the thermal energy carried by these molecules, a physical process that was well characterized by Einstein[1]. In a free medium, during a given time interval, molecular displacements obey a three-dimensional Gaussian distribution — molecules travel randomly in space over a distance that is statistically well described by a diffusion coefficient (D). This coefficient depends only on the size (mass) of the molecules, the temperature and the nature (viscosity) of the medium. For example, in the case of 'free' water molecules diffusing in water at 37 °C, the diffusion coefficient is 3×10^{-9} m^2 s^{-1}, which translates to a diffusion distance of 17 μm during 50 ms (FIG. 1a) — about 32% of the molecules have moved at least this distance, whereas only 5% of them have travelled over distances greater than 34 μm.

dMRI is deeply rooted in the concept that, during their diffusion-driven displacements, molecules probe tissue structure on a microscopic scale, well beyond the usual (millimetric) image resolution. During typical diffusion times of about 50–100 ms, water molecules move in brain tissues, on average, over distances of

Anatomical and Functional Neuroimaging Laboratory, Service Hospitalier Frédéric Joliot, Commissariat à l'Energie Atomique, and Federative Institute of Functional Neuroimaging (IFR 49), 4 place du General Leclerc, 91401 Orsay, France. e-mail: lebihan@shfj.cea.fr
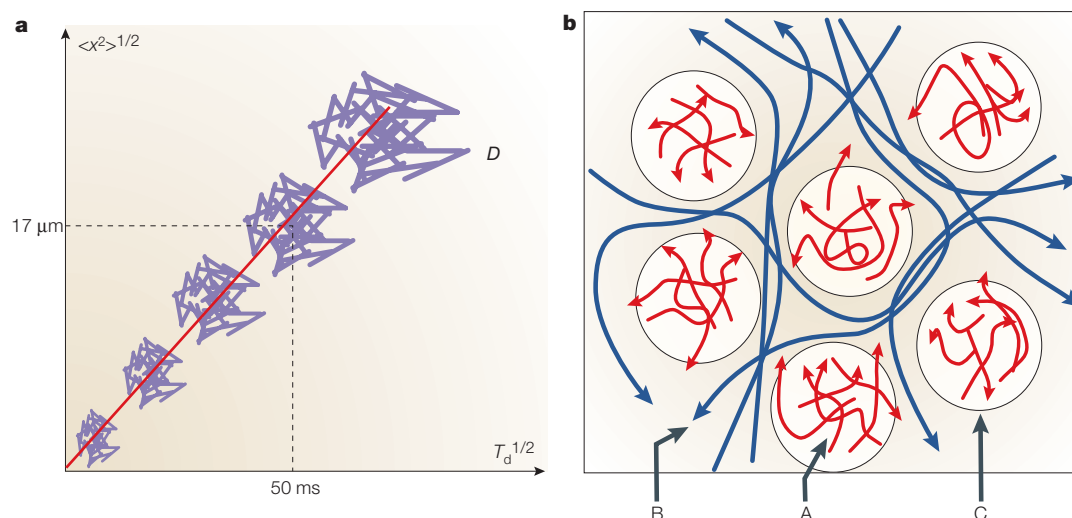
Figure 1 | **Water diffusion and tissue microstructure. a** | The random displacements of molecules resulting from thermal agitation (Brownian motion) obey a statistical law established by Einstein in 1905. Along one dimension in space, $<x^2> = 2DT_d$, where T_d is the time for molecules to diffuse (diffusion time), D is the diffusion coefficient and $<x^2>$ is the variance of the molecular displacement along that dimension. With a very large number of molecules, the size of the 'cloud' representing average molecular excursion (root-mean-square of $<x^2>$) increases linearly with the square root of T_d. For water at brain temperature, 68% of molecules have moved within a sphere of 17 μm diameter in 50 ms. **b** | In biological tissues, obstacles modulate the free diffusion process. Diffusion of molecules can be restricted in closed spaces (A), such as cells. Diffusion might also be hindered by obstacles that result in tortuous pathways (B). Exchange between compartments also slows down molecular displacements (C). So, the apparent diffusion coefficient, ADC, is usually reduced compared with D, but closely reflects tissue microstructure.

around 1–15 μm, bouncing off, crossing or interacting with many tissue components, such as cell membranes, fibres and macromolecules. (The diffusion of other molecules can also be detected; see BOX 1.) Because movement of water molecules is impeded by such obstacles (FIG. 1b), the actual diffusion distance is reduced compared with that of free water, and the displacement distribution is no longer Gaussian. In other words, although short diffusion times reflect the local intrinsic viscosity, at longer diffusion times the effects of the obstacles predominate. So, the non-invasive observation of the water diffusion-driven displacement distributions *in vivo* provides unique clues to the fine structural features and geometric organization of neural tissues, and also to changes in these features with physiological and pathological states.

Imaging diffusion with MRI

Principles. Although early water diffusion measurements were made in biological tissues using NMR in the 1960s and 1970s, it was not until the mid-1980s that the basic principles of dMRI were laid out[2–4] (see REF. 5 for a review). In the 1970s and 1980s, the introduction of MRI made it possible to see the anatomy of the brain *in vivo* with an exquisite (submillimetric) spatial resolution. This advance relied on the ability to physically manipulate, through electromagnetic radiowaves, the tiny magnetization of water hydrogen nuclei of the brain that is induced in a strong, homogeneous magnetic field[6]. The contrast underlying anatomical MRI results from the 'relaxation times', called T1 and T2, that characterize how fast water magnetization returns to equilibrium after the perturbation induced by the electromagnetic waves, which depends roughly on the nature of the tissue.

By combining MRI principles[7] with those introduced earlier in NMR physics and chemistry to encode molecular diffusion effects, it became possible to obtain local measurements of water diffusion *in vivo* in the whole human brain. Magnetic resonance signals can be made sensitive to diffusion through the use of a pair of sharp magnetic field gradient pulses[8], the duration and the separation of which can be adjusted. In an otherwise homogeneous field, the first pulse magnetically 'labels' hydrogen nuclei (or protons) that are carried by water molecules according to their spatial location, as, for a short time, the magnetic field slowly varies along one direction (FIG. 2). The second pulse is introduced slightly later to detect the changes in the location of nuclei; that is, the displacement history of nuclei that occurred during the time interval (or 'diffusion time') between the two pulses. A change in location (along the gradient direction) of a hydrogen nucleus carried by a diffusing water molecule results in a change of the magnetic field 'seen' by this nucleus, which is proportional to the displacement. Considering now a population comprising a large number of diffusing water molecules, the overall effect is that the corresponding hydrogen nuclei will experience various magnetic field changes that closely reflect the statistical displacement distribution of this population; that is, the statistical diffusion process. This variation of the magnetic field seen by the population of nuclei results in an MRI radiowave signal that is slightly less than that obtained from a population of nuclei that is placed in a perfectly homogeneous field. This signal attenuation is precisely and quantitatively linked to the degree of magnetic field broadening, and hence to the amplitude of the displacement distribution — fast (slow) diffusion results

Box 1 | Diffusion of non-water molecules and metabolites

Water might not be the most suitable molecule for diffusion measurements in biological tissues owing to its ubiquity and to the permeability of most tissue interfaces, such as membranes, to water molecules. For instance, diffusion of *N*-acetylaspartate and myoinositol might provide more useful information about neuronal and glial cell populations, respectively. So, diffusion measurements of larger molecules that are more tissue- or compartment-specific are more promising tools for tissue characterization. However, such measurements are technically challenging compared with diffusion measurements of water molecules because of the low concentration of the larger molecules and their relatively low diffusion coefficients. Data on magnitudes and even directional ANISOTROPY of diffusion coefficients of molecules such as choline, creatine/phosphocreatine and *N*-acetylaspartate in animals[137] and in human brain[138] have been made available. In the expanding field of 'molecular (or cellular) imaging', measurements of metabolite diffusion could provide valuable information about intracellular content and machinery; although water could diffuse easily in small spaces between small obstacles such as organelles or macromolecules, larger metabolites would not fit within these spaces. Such considerations should be useful in understanding how diffusion of intracellular metabolites, such as *N*-acetylaspartate, decreases in the acute phase of brain ischaemia[139]. On the other hand, diffusion is not the only source of movement within cells. Other flowing patterns, such as cytosolic streaming, must be considered — the flow of large molecules carried by this active stream would artificially contribute to the apparent diffusion coefficient (ADC), reflecting the overall flow rather than individual molecular diffusion. Such a model would be compatible with the observation that metabolites of different sizes have similar diffusion coefficients[138] and that the intracellular ADC decreases on cell death[139]. Recent results in oocytes[140] do not confirm this view, but such large cells might not be a good representation of neurons, especially those in neuronal tissues where interactions between intracellular and intercellular spaces are complex.

Figure 2 | **Principles of diffusion magnetic resonance imaging (dMRI).** In the presence of a spatially varying magnetic field (induced through a magnetic field gradient, the amplitude and timing of which are characterized by a '*b*' factor), moving molecules emit radiofrequency signals with slightly different phases. In a small volume (voxel) containing a large number of diffusing molecules, these phases become randomly distributed, directly reflecting the trajectory of individual molecules (that is, the diffusion process). This diffusion-related phase distribution of the signal results in an attenuation of the MRI signal. This attenuation (*A*) quantitatively depends on the gradient characteristics (embedded in the *b* factor) and the diffusion coefficient (*D*), according to $A = e^{-bD}$. As diffusion effects are small, large gradient intensities must be used, which requires special MRI hardware.

in a large (small) distribution and a large (small) signal attenuation. Of course, the effect also depends on the intensity of the magnetic field gradient pulses. It is important to note that only the displacement (diffusion) component along the gradient direction is detectable.

In practice, any MRI technique can be sensitized to diffusion by inserting the adequate magnetic field gradient pulses[9]. By acquiring data with various gradient pulse amplitudes, images with different degrees of diffusion sensitivity are obtained (FIG. 3). Contrast in these images depends on diffusion but also on other MRI parameters, such as water relaxation times. So, these images are often numerically combined to determine, using a global diffusion model, an estimate of the diffusion coefficient in each image location. The resulting images are maps of the diffusion process and can be visualized using a quantitative scale (FIG. 3).

Diffusion and tissue microstructure: a scaling issue. One must bear in mind, however, that the overall signal observed in a dMRI image volume element (voxel), at a millimetric resolution, results from the integration, on a statistical basis, of all the microscopic displacement distributions of the water molecules present in this voxel. As a departure from earlier biological diffusion studies, in which efforts were made to depict the true diffusion process[10–12], it was suggested[13] that the complex diffusion processes that occur in a biological tissue be portrayed on a voxel scale using the microscopic, free-diffusion physical model, but replacing the physical diffusion coefficient, *D*, with a global, statistical

parameter, the apparent diffusion coefficient (ADC). The ADC concept has since been largely used in the literature. This parameterization of the diffusion process by a global ADC is similar to the step followed by meteorologists to describe atmospheric processes on a scale (parcel) that is large when compared with that of the local physical processes[14]. Parameterization is intended to represent physical processes that occur on scales smaller than those resolved by the method — the large scale is imposed by technical limitations (for example, large distances between weather measurement stations), whereas the actual 'theatre' scale of the physical elementary processes (for example, cloud microphysics) is determined by natural/physical phenomena. Parameterization models allow us partially to bridge the gap between the two scales.

ANISOTROPY
The characteristic of a medium in which physical properties have different values when measured along axes orientated in different directions.
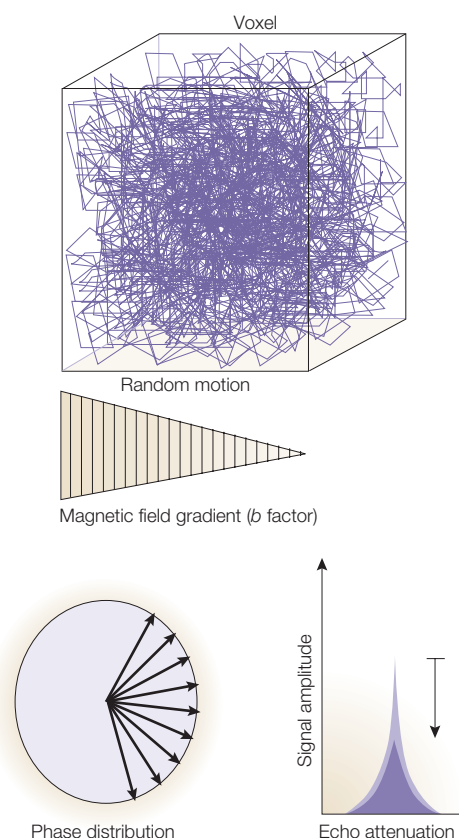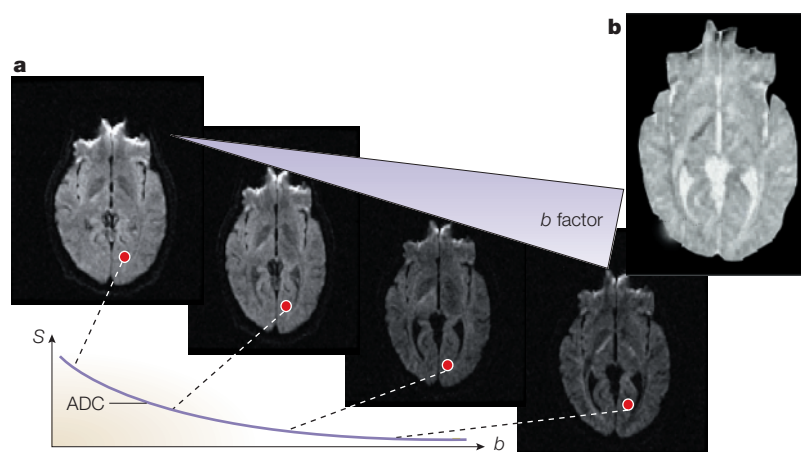
Figure 3 | **Diffusion-weighting.** In practice, different degrees of diffusion-weighted images can be obtained using different values for the *b* factor (**a**). The larger the *b* factor, the more the signal intensity (*S*) becomes attenuated in the image. This attenuation is modulated by the diffusion coefficient — the signal in structures with fast diffusion (for example, water-filled ventricular cavities) decays rapidly with increasing *b*, whereas the signal in tissues with low diffusion (for example, grey and white matter) decreases more slowly. By fitting the signal decay as a function of *b*, one obtains the apparent diffusion coefficient (ADC) for each elementary volume (voxel) of the image. Calculated diffusion images (ADC maps) that depend solely on the diffusion coefficient can then be generated and displayed using a grey (or colour) scale. High rates of diffusion — as in the ventricular cavities — appear as bright areas, whereas areas with low rates of diffusion are dark (**b**).

Regarding MRI, microscopic imaging is possible, but requires scanners with strong magnetic fields and gradient systems that are available for animal studies only. In the case of dMRI, the image resolution becomes limited by the water diffusion process itself, which introduces some blurring in the images[15]. With most current systems, especially those developed for human applications, the voxel size remains large (a few mm³). The averaging, smoothing effect resulting from this scaling assumes some homogeneity in the voxel and makes a direct physical interpretation from the global parameter difficult, unless some assumptions are made. The ADC now depends not only on the actual diffusion coefficients of the water molecule populations present in the voxel, but also on experimental, technical parameters, such as the voxel size and the diffusion time. The relationship between the ADC and specific tissue microscopic features is now the object of intensive research. However, as in meteorology, parameterization remains a powerful concept, as long as the scale is well defined and limitations are kept in mind.

dMRI and acute brain ischaemia. Although the first diffusion images of the brain were obtained in the mid-1980s, both in normal subjects and in patients[13], it was not until the mid-1990s that dMRI really took off. Initially, the specifications of the clinical MRI scanners made it difficult to obtain reliable diffusion images, as acquisition times were long (10–20 minutes) and the presence of the large gradient pulses required for diffusion also made the images sensitive to macroscopic motion artefacts, such as those induced by head motion, breathing or even cardiac-related brain pulsation[16]. Therefore, although dMRI was shown to be

potentially useful in the clinic, demonstrative clinical studies started later, when better MRI scanners equipped with echo-planar imaging (EPI) became available. With standard MRI, images are acquired in several pieces over periods of seconds or minutes, which makes this method particularly susceptible to errors introduced by head motion. By exploiting gradient hardware, EPI makes it possible to collect a brain image at once, in a single 'shot' lasting a few tens of milliseconds, and images of the whole brain in less than a second, virtually freezing macroscopic motion.

The most successful application of dMRI since the early 1990s has been in acute brain ischaemia[17]. The application of dMRI to patients with chronic infarct lesions was suggested early in the development of this technique[13,18]. However, an important discovery was made later by Moseley *et al.*[19,20] when they demonstrated that the water diffusion coefficient decreases significantly (by 30–50%) in ischaemic brain tissue within several minutes of occlusion of the middle cerebral artery in the cat. This finding was soon confirmed by several groups using other animal models (see REFS 21,22 for extensive reviews) and later in human patients with stroke[23–25] (FIG. 4). By contrast, T2-weighted images of ischaemic tissue remain normal for several hours. An increase in T2 occurs later, when VASOGENIC OEDEMA develops[26]. Now, dMRI is the imaging modality of choice for the management of stroke patients. However, although the decrease in water diffusion immediately after ischaemic injury has been clearly established, its interpretation is still incomplete, and its relationship to the severity of ischaemic damage and clinical outcome is still a subject of study[22]. Decreased diffusion is linked to the cellular change in energy metabolism that ultimately leads to the decreased activity and subsequent failure of the Na^+/K^+ pumps, which in turn result in CYTOTOXIC OEDEMA[21]. The basic mechanism underlying the decrease in diffusion remains unclear. Different hypotheses have been evaluated, such as a possible decrease in the extracellular and intracellular water mobility, a shift of water from extracellular to intracellular spaces, an increase in restriction of intracellular diffusion due to changes in membrane permeability, or increased tortuosity in the extracellular space due to cell swelling[27]. Regardless, diffusion imaging has great potential in the management of stroke patients. First, the development of pharmaceuticals for the treatment of stroke can be greatly facilitated by dMRI, as drug effects can be assessed objectively and quickly compared with long and costly clinical trials or animal model studies. dMRI used in combination with perfusion MRI (which outlines regions with decreased blood flow or increased blood mean transit times[28]) and magnetic resonance 'angiography' (which provides images of the vasculature, showing occluded vessels) is an invaluable tool for the assessment of lesion severity and extension at an early stage when tissue is still salvageable. These methods should also allow clinicians to customize therapeutic approaches (pharmacological or interventional) for individual patients[29], as well as to monitor patient progress on an objective basis (in both the acute and the chronic phase[30]) and to predict clinical outcome[31–34].

VASOGENIC OEDEMA
The accumulation of extracellular fluid that results from changes in capillary permeability, allowing the seepage of plasma molecules and water.

CYTOTOXIC OEDEMA
The swelling of cellular elements and reduction in extracellular space that are commonly associated with anoxia and ischaemia. The underlying mechanism is a failure of the ATP-dependent Na^+/K^+ pumps, and the subsequent accumulation of intracellular sodium and water. In contrast to vasogenic oedema, capillary permeability is not impaired in cytotoxic oedema.
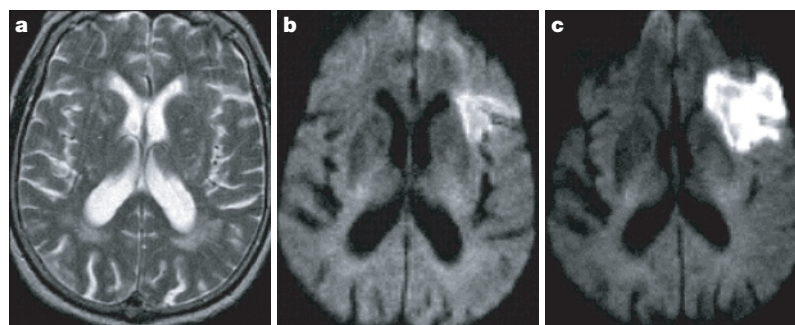
Figure 4 | **Acute brain ischaemia.** An important clinical application of diffusion magnetic resonance imaging (MRI) is in the detection and characterization of acute brain ischaemia. Images (**a**, conventional MRI; **b**, diffusion-weighted) were obtained 3 hours after the onset of aphasia in a female patient. The diffusion image shows the infarcted tissue with an intense signal corresponding to reduced water diffusion in the ischaemic territory. Five days later the lesion is more severe and extended (**c**). Images courtesy of A. G. Sorensen. Reproduced, with permission, from REF. 25 © (1999) The Radiological Society of North America.

Current limitations. Although the EPI technique is the method of choice for *in vivo* diffusion imaging, it is susceptible to certain artefacts. EPI requires a homogeneous magnetic field. Magnetic interfaces between bone or air-filled cavities (sinuses) and water-containing tissues result in local image distortion or signal dropout[35]. Also, the spatial resolution of EPI is often coarse (around 2 mm) owing to hardware limitations. Recently developed 'parallel' acquisition techniques, which allow signals to be collected simultaneously using an array of radiofrequency coils, may be able to correct for these limitations[36,37]. Another point is that the minimum length of detectable molecular diffusion paths is determined primarily by the intensity of the gradient pulses. Therefore, there is a need to use hardware that can provide stable gradients of the utmost intensity[38]. Although this requirement can be satisfied with small-bore MRI scanners that are dedicated to small animals (delivering gradient intensities of up to 1,000 mT m^{-1}), it becomes extremely challenging in terms of electrical power supply when considering whole-body instruments for human studies. As a consequence, magnetic gradient pulses must have a finite, non-negligible duration to produce measurable diffusion sensitization, loosely defined because diffusion effects occurring during the presence of the pulses introduce some blurring. With clinical systems, diffusion displacements below a few micrometres are impossible to attain. Furthermore, on the biological/ safety side, strong gradient pulses cannot be switched rapidly, as they might induce currents in tissues that can depolarize sensitive cells and become harmful. Also, gradient switching inside the main magnet causes the gradient hardware to vibrate, generating loud sounds that can easily exceed 100 dB.

Diffusion and brain activation

The number of articles published that deal with functional MRI (fMRI) has soared during the past ten years. In fMRI, neuroscientists have a powerful tool to see the brain at work — and, to some extent, to see the workings of the mind — by showing cortical regions that are activated by different cognitive processes. However, the key concept behind blood oxygenation level dependent (BOLD) fMRI[39] is the indirect (and still poorly understood) link between local blood flow and neuronal activity[40]. Brain activation is visualized with fMRI through a haemodynamic window; there is a delay of several seconds between the visible haemodynamic response and the onset of the neuronal response, which intrinsically limits the temporal resolution of the method. Similarly, spatial resolution is limited, because the vessels at the origin of the present fMRI response feed or drain large territories compared with the activated neuronal assemblies. Typical image resolution for fMRI is around 1–3 mm and 1–3 s.

Preliminary data have indicated that water dMRI could be used to visualize changes in tissue microstructure that might arise during large, extraphysiological neuronal activation[41]. Changes in the water ADC during neuronal activation would probably reflect transient microstructural changes of the neurons or the glial cells during activation. Observing such effects would have a tremendous impact on the imaging of brain activation, as they would be directly linked to neuronal events, in contrast to blood flow effects, which are indirect and remote. Recently, a transient decrease in the ADC of water has been reported in the visual cortex of the human brain during activation by a flickering black-and-white checkerboard[42]. The decrease in ADC was small (less than 1%), but significant and reproducible, and closely followed the time course of the activation experiment (FIG. 5). Based on the known sensitivity of dMRI to cell size in tissues and on optical imaging studies that have revealed changes in the shape of neurons and glial cells during activation, these ADC findings have been tentatively ascribed to a transient swelling of cortical cells.

Early studies based on optical measurements in animal preparations identified an early change in photon scattering, which occurs immediately at the onset of the stimulation[43]. Although the mechanisms of these changes in photon scattering have not been fully elucidated, changes in neuronal volume, especially at the axon hillock, have been proposed as one mechanism. More recent optical imaging techniques in tissue preparations and *in vivo* have confirmed that there are intrinsic regional changes in light transmittance during stimulation of synaptic pathways, which can be attributed to cell swelling at the site of action potential initiation[44]. Interestingly, it seems that this swelling also involves dendrites and glial cells, although the mechanisms might be different[45] and the changes might last longer for glial cells[46]. It is also worth noting that contractile proteins that are associated with dendritic spines (where the majority of synapses are located in the cerebral cortex) could allow these spines to change shape rapidly during neuronal activity[47,48]. However, these spines occupy a small volume fraction.

These preliminary results highlight a new approach to producing images of brain activation with MRI from signals that are directly associated with neuronal activation, rather than through changes in local blood flow.
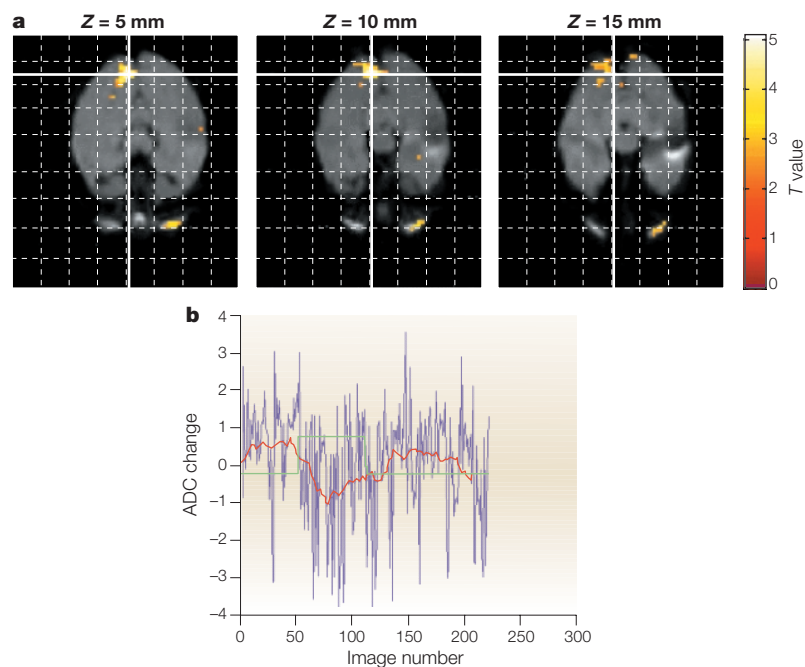
Figure 5 | **Water diffusion and brain activation. a** | In a recent study[42], a transient decrease in the apparent diffusion coefficient (ADC) was observed in human visual cortex locked to visual stimulation. Statistical parametric maps (T statistics) show, in colour pixels, the decrease in ADC. **b** | On the basis of physiology and the optical imaging literature, this small (about 1%) but statistically significant decrease in water mobility has been tentatively ascribed to transient swelling of activated cortical cells (graph shows ADC time course (blue) and moving average (red) in the visual cortex during the presentation of a visual stimulus (green)). This finding might lead to the direct detection of neuronal activity, as opposed to detection through the local modulation of cerebral blood flow.

Diffusion anisotropy in white matter

The diffusion tensor. Diffusion is a three-dimensional process, and water molecular mobility in tissues is not necessarily the same in all directions. This diffusion anisotropy might result from the presence of obstacles that limit molecular movement in some directions. Slight anisotropic diffusion effects were observed in biological tissues during early studies, especially in tissues with strongly orientated components, such as excised rat skeletal muscles[49,50]. However, it was not until the advent of dMRI, at the end of the 1980s, that anisotropy was detected for the first time *in vivo* in spinal cord and brain white matter[51,52]. Diffusion anisotropy in white matter originates roughly from the specific organization of this tissue as bundles of more or less myelinated axonal fibres running in parallel; diffusion in the direction of the fibres (whatever the species or the fibre type) is about three to six times faster than in the perpendicular direction (FIG. 6). However, the relative contributions to the ADC of the intra-axonal and extra-cellular spaces, and the myelin sheath, as well as the exact mechanism of anisotropy, are still not completely understood and remain the object of active research (see REF. 53 for a recent review). It quickly became apparent, however, that this anisotropy effect could be exploited to map the orientation in space of the white matter tracks in the brain, assuming that the direction of fastest diffusion would indicate the overall orientation of the fibres[54]. Work on diffusion anisotropy became prevalent with the introduction of the more rigorous formalism of the diffusion tensor by Basser *et al.*[55,56]. In diffusion tensor imaging (DTI), diffusion is no longer described by a single diffusion coefficient, but by an array of nine coefficients that fully characterize how diffusion in space varies according to direction (see REF. 57 for a recent review on DTI). So, diffusion anisotropy effects can be fully extracted and exploited, providing even more exquisite detail on tissue microstructure. As it is difficult to display tensor data, the concept of 'diffusion ellipsoids' has been conveniently proposed[55,56]. An ellipsoid is a three-dimensional representation of the diffusion distance covered in space by molecules in a given diffusion time. In the case of isotropic diffusion, the ellipsoid is simply a sphere, the size of which is proportional to the diffusion coefficient. In the case of anisotropic diffusion, the ellipsoid becomes elongated (cigar-shaped) if one diffusion direction predominates, or flat (pancake-shaped) if one direction contributes less than the others.

In DTI, diffusion data can be analysed in three ways to provide information on tissue microstructure and architecture for each voxel[5,58]. First, the mean diffusivity, which characterizes the overall mean-squared displacement of molecules (average ellipsoid size) and the overall presence of obstacles to diffusion. Second, the degree of anisotropy, which describes the degree to which molecular displacements vary in space (ellipsoid eccentricity) and is related to the presence and coherence of orientated structures. And third, the main direction of diffusivities (main ellipsoid axes), which is linked to the orientation in space of the structures (FIG. 7). These three DTI 'meta-parameters' can be derived from a complete knowledge of the diffusion tensor or some of its components. For instance, in stroke, the average diffusion and the diffusion anisotropy in white matter have different time courses, enhancing the potential for the use of dMRI in accurate diagnosis and prognosis of stroke[22].

Many studies have been published that deal with the optimization of MRI sequences that are necessary to gain access to the diffusion tensor, the processing and display of DTI data[59,60], and potential applications. The most advanced application is that of fibre tracking in the brain, which, in combination with fMRI, might open a window on the important issue of connectivity. Whereas fMRI provides information about the cortical areas involved in a given cognitive process, connectivity studies generate information on the structural/dynamic wiring that determimes how those areas are networked. In the clinical field, some psychiatric disorders have been linked to connectivity dysfunction. Anatomical and functional MRI may appear normal in those patients, although dysconnectivity might be revealed by DTI.

The origin of water diffusion anisotropy. The concepts of restriction, hindrance or tortuous displacements around multiple physical compartments (FIGS 1b and 6) are particularly useful in understanding diffusion in brain white matter[5]. The facts are that, first, water diffusion is highly anisotropic in white matter[52,61,62]; second, anisotropy has been observed even before fibres are myelinated, although to a lesser degree[63–70]; and third, ADCs that are
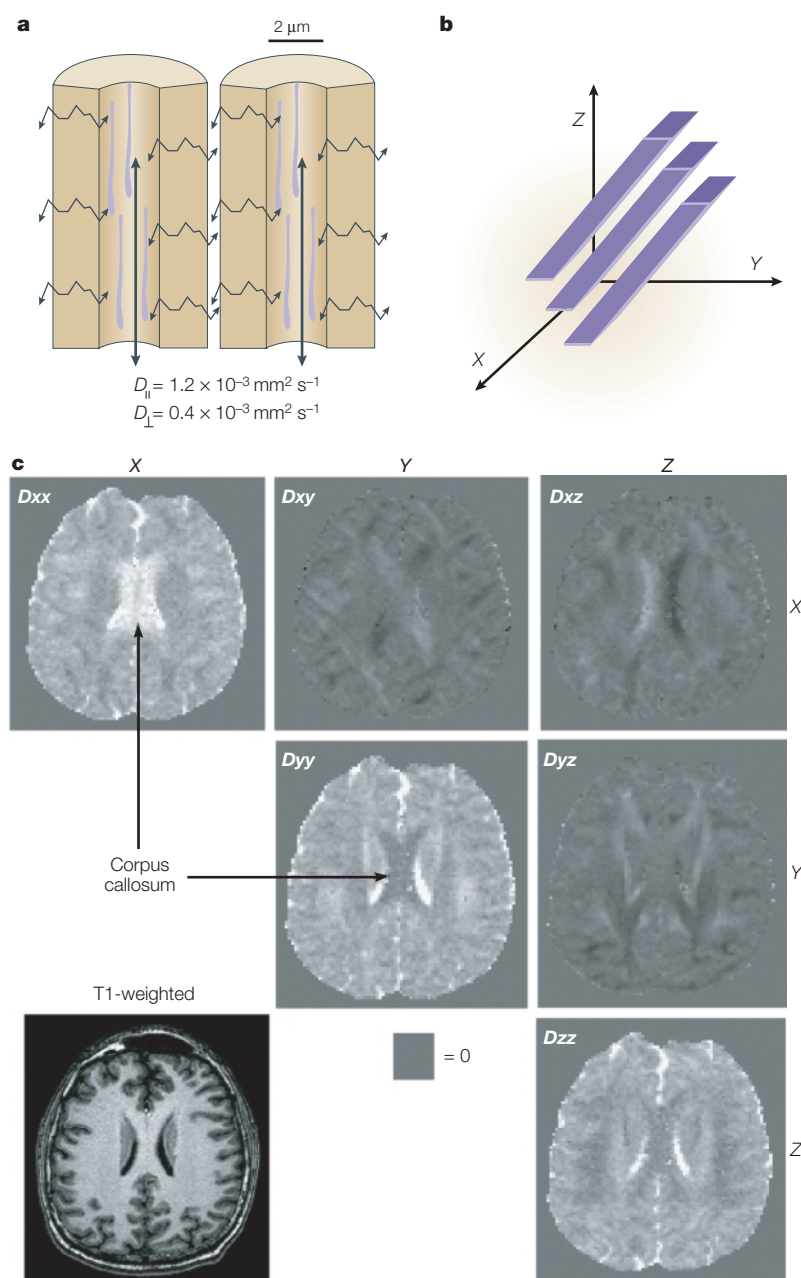
Figure 6 | **Anisotropic diffusion. a** | Water mobility is not always the same in all directions. In brain white matter, for instance, water diffusion anisotropy is directly related to the organization of white matter as bundles of parallel fibres. In both intra-axonal and interstitial compartments, molecular displacements of a few microns are hindered to a greater degree when they are perpendicular ($D_\perp$), rather than parallel ($D_\parallel$), to the fibres. As a result of this decreased water mobility, the apparent diffusion coefficient (ADC) is smaller when measured perpendicular to the main fibre direction than when measured in the direction of the fibre bundle. **b** | In the case of anisotropy, diffusion is more adequately characterized by a diffusion tensor, as opposed to a diffusion coefficient. **c** | The diffusion tensor is an array of numbers that describes mobility in perpendicular directions (*Dxx*, *Dyy*, *Dzz*), as well as coupling between different directions (*Dxy*, *Dxz*, *Dyz*). The corpus callosum has high diffusion on a *Dxx* map and low diffusion on *Dyy* and *Dzz* maps, because fibres run mainly transversely (the *x* axis is aligned with right/left direction, the *y* axis with anterior/posterior direction and the *z* axis with inferior/superior direction). The *Dxz* map shows the interaction between the vertical and the transverse direction of the fibres; in the corpus callosum, the areas of high and low diffusion that are visible in the left and right part of the image centre, respectively, reflect the fact that right and left fibres are almost perpendicular to each other. Similarly, in the *Dxy* map the appearance of the anterior and posterior parts of the corpus callosum in the left and right hemispheres reflects fibre orientations with respect to a direction at 45° to the *x* and *y* axes.

measured parallel and perpendicular to the fibres do not seem to depend on diffusion time[71–73], at least for diffusion times longer than 20 ms.

Initial reports indicated that anisotropic water diffusion could be explained by the restriction of water molecules in axons (anisotropically restricted diffusion) owing to the presence of the myelin sheath[74,75]. Restricted diffusion of intra-axonal metabolites, such as *N*-acetylaspartate, has been observed (BOX 1), as has restricted diffusion of truly intra-axonal water[76]. However, this effect probably accounts for only a limited part of the whole picture, as 'true' restriction patterns have not been observed for water diffusion in white matter *in vivo*. Extracellular water might also contribute to the anisotropy effect; when diffusing perpendicular to the fibres, water molecules must travel along tortuous pathways around fibres, which slows their rate of movement[71]. Also, the packed, parallel arrangement of the fibres might be sufficient to explain the presence of anisotropy before myelination, although to a lesser degree than after myelination. It is unlikely that axonal transport significantly contributes to water diffusion anisotropy, considering its low velocity. Likewise, neurofilaments within axons do not seem to play any part in anisotropy. Experimental evidence indicates the importance of the spatial organization of membranes. Myelin is not required to generate diffusion anisotropy, but it might modulate the degree of anisotropy.

The issue, then, is to determine the respective contributions of the extracellular and intracellular compartments to the measured ADC. With the use of stronger magnetic field gradient pulses, it became clear that water diffusion that was measured in tissues, including brain white matter, could not be described in terms of a single diffusion coefficient, as modelled by the ADC. Models including multiple (usually two) compartments with some degree of exchange have been developed. Results obtained by independent groups using this model are quantitatively similar and compatible with the existence of two water diffusion 'pools', one fast, the other slow. The physical origin of these pools remains a mystery. Assignment of the fast- and slow-diffusing pools to the extracellular and intracellular compartments, respectively, is tempting[77], but it is unclear why their respective contributions to the ADC do not match the expected biological extracellular and intracellular volume fractions (82.5 and 17.5%, respectively). Other compartments might be considered; for instance, inside the cells, in axons or in myelin[70]. Under certain conditions, the presence of restrictive barriers in a single-compartment system can lead to quasi-two-compartment behaviour of the magnetic resonance signal[78]. Simulation of the diffusion process shows that water molecules near tissue boundaries (for example, cell membranes) seem to 'stick' to these boundaries, which results in an artificially decreased diffusion coefficient. Here, also, it seems that the density and the spatial arrangement of the membranes have determinant roles. The correct assignment of water diffusion patterns to the underlying tissue microarchitecture is a challenging task.
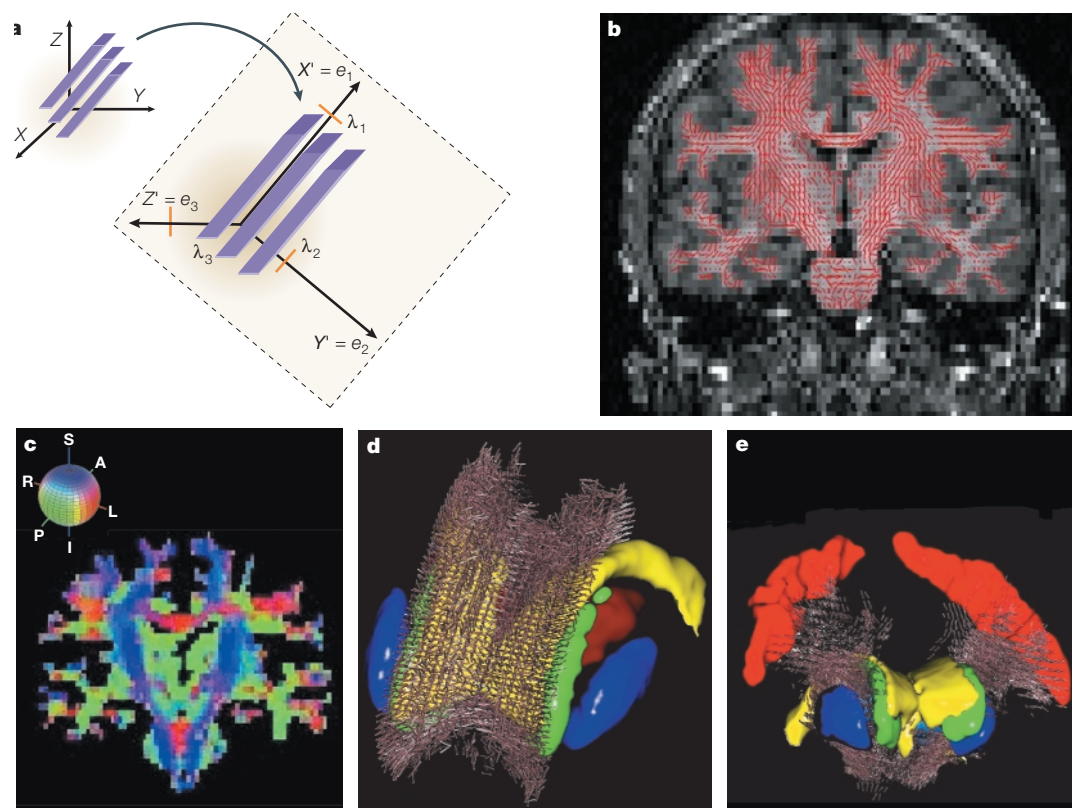
Figure 7 | **Fibre orientation. a** | Assuming that the direction of higher diffusion in each image voxel in the magnetic resonance imaging frame {X, Y, Z} indicates the main fibre orientation, it is possible to determine, on a voxel-by-voxel basis, the virtual reference frame {X', Y', Z'} that is aligned with the fibres through the diagonalization of the diffusion tensor. The diffusion values in the new directions {e_1, e_2, e_3} are now {λ_1, λ_2, λ_3}, and are used to produce white matter fibre-orientation maps. Orientation can be displayed using vector pointers (**b**), colour scales (**c**) or three-dimensional segments (**d**, **e**). Images courtesy of J. F. Mangin and C. Poupon, Service Hospitalier Frédéric Joliot, Commissariat à l'Energie Atomique. A, anterior; I, inferior; L, left; P, posterior; R, right; S, superior.

Although the exact mechanism of diffusion anisotropy is not well understood, this anisotropy directly reflects the presence of spatially orientated structures in the tissue. The degree of anisotropy, as measured by the various anisotropy indices that have been proposed in the literature, is linked in some way to the integrity and the density of orientated structures in the tissue.

Brain connectivity. Studies of neuronal connectivity are important in the interpretation of fMRI data and in the identification of the networks that underlie cognitive processes. Detailed knowledge of the anatomical connections (in terms of length and size of the fibres, as obtained from the diffusion tensor measurements) might also provide information about the propagation times between activated foci and, so, might indirectly provide clues to the timing of the activation of each node in the network. This type of information would be particularly useful when exploring synchronizations between cortical regions.

Basic DTI provides a means to determine the overall orientation of white matter bundles in each voxel, assuming that only one direction is present or predominant in each voxel and that diffusivity is greatest in this direction. Three-dimensional vector field maps representing fibre orientation in each voxel can then be obtained from the image data through the diagonalization (a mathematical operation that provides orthogonal directions that coincide with the main diffusion directions) of the diffusion tensor that is determined in each voxel. A second step after this 'inverse problem' is solved is to connect subsequent voxels on the basis of their respective fibre orientation, to infer some continuity in the fibres. Several algorithms have been proposed (see REF. 79 for a review). Line-propagation algorithms reconstruct tracts from voxel to voxel from a seed point[80,81]. Another approach is based on regional energy minimization (minimal bending) to select the most probable trajectory from several possibilities[82] (FIG. 8). Colour maps showing 'virtual' fibre bundles across the brain, which can now be easily produced, regularly make the cover of imaging journals. Interestingly, significant progress is made not so much through MRI physics, but through insights from modern, powerful image-processing methods used in other fields (for example, 'spin glass models'[83]). Another trend is to match functional connectivity obtained with fMRI and anatomical connectivity inferred from DTI[84]. In any case, one must bear in mind that, at this stage, only white matter bundles composed of large number of axons are visible (intracortical connections are not), and that there is no indication of the directional and functional status
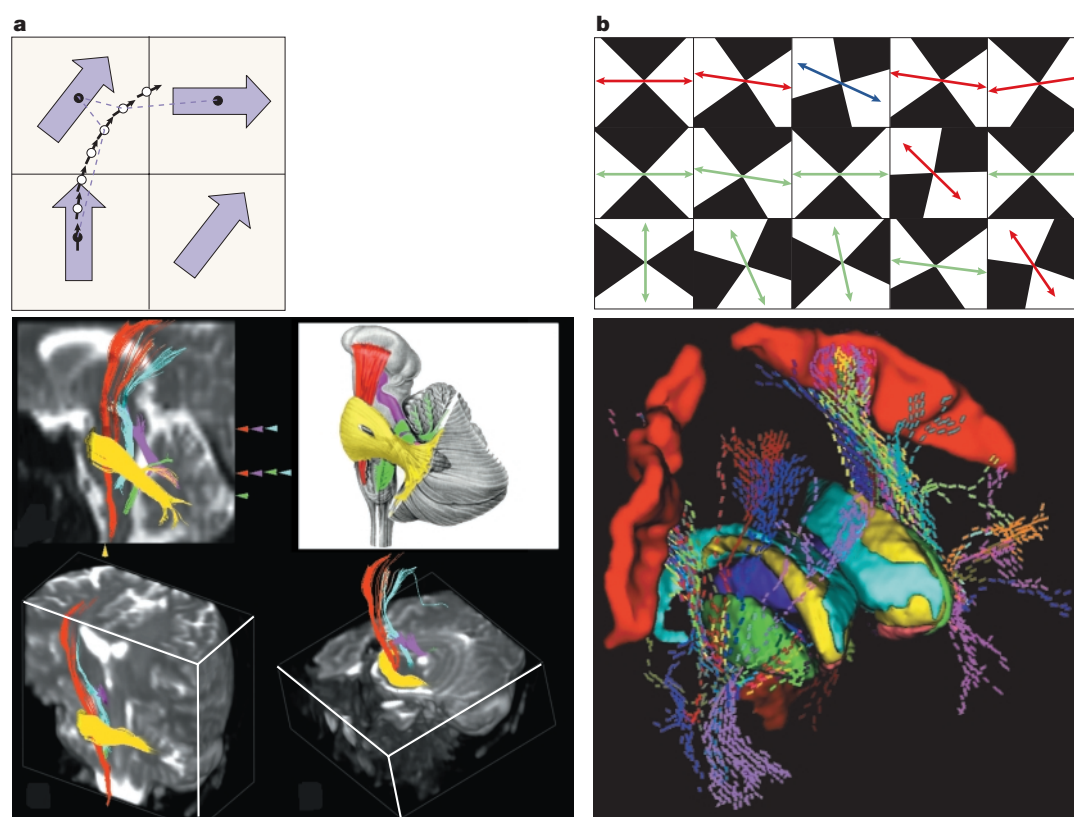
Figure 8 | **Fibre tracking: connecting voxels.** Several approaches have been developed to connect voxels after white matter fibres have been identified and their orientation determined. **a** | With the FACT (fibre assignment by continuous tracking) algorithm[80], tracking is performed on a voxel-by-voxel basis. The overall track is determined from a seed point, following the successive orientations associated with adjacent voxels. Images courtesy of S. Mori and P. van Zijl, Johns Hopkins University School of Medicine. **b** | Regularization methods allow local patterns of fibre stiffness to be taken into account[82]. Voxels with uncertain orientation (blue) can then be included or excluded from tracks, depending on the allowed degree of curvature of the tracks. Images courtesy of J. F. Mangin and C. Poupon, Service Hospitalier Frédéric Joliot, Commissariat à l'Energie Atomique.

of the information flow along the tracts. Whether MRI will some day be able to provide such crucial information remains to be established.

Validation of virtual bundles against actual anatomical data has not been achieved, even in animal models. In fact, there are no such data, as there are no means to obtain entire fibre bundle pathways from dissections. Fibres can be labelled and seen *in vitro* using the peroxidase uptake method, but only over a short range because of the way in which tissues must be processed for microscopy. The combination in animal models of DTI and fibre tracking using manganese as a contrast agent that is actively taken up by neurons is a breakthrough that will help to validate DTI[85]. Group analysis, for instance, using tools such as VOXEL-BASED MORPHOMETRY (VBM)[86,87] could highlight common features and differences across subjects in a given population. This approach will be useful, not only to assess the robustness of DTI, but also to establish atlases of white matter anisotropy, or even bundles, which are currently lacking. However, the VBM approach still faces difficulties, especially with regard to brain normalization and segmentation processes.

There are important circumstances in which the diffusion tensor approach fails. The 'one bundle–one

orientation' assumption is acceptable for the main, large tracts, but becomes unrealistic in regions where several fibre tracks with different orientations cross, diverge or converge. In these situations, the basic tensor formalism is inadequate. For instance, with two bundles crossing at a right angle in a voxel, the largest diffusivities are measured at 45° to the actual bundle directions. This is a problem that requires improvements to the diffusion tensor model, or the development of new strategies. Among such strategies, the direct processing (bypassing the tensor calculation) of diffusion-weighted images acquired with a high angular resolution (through diffusion measurements along many directions) has proved successful[88–90], although acquisition times are still long. By increasing the spatial resolution of images, averaging effects over the different orientations in each voxel might be reduced, as fewer fibre bundles will be present in smaller voxels. But there will always be regions where fibres of different bundles travel together. This poses the question of the ultimate spatial resolution that can be achieved with dMRI. There must be some degree of anisotropy for the tracking algorithms to work and, so far, most algorithms stop short of the brain cortex, where diffusion anisotropy is greatly reduced. However, recent data at high resolution in animals[91] and humans[64] show

VOXEL-BASED MORPHOMETRY
A technique that uses a voxel-by-voxel comparison of the local concentration of grey and white matter between different groups of subjects. It involves the spatial normalization of the images to the same stereotactic space, segmenting the grey and white matter, smoothing the segments, and comparing the smoothed images between the groups.

grey matter structure. Although such data must be viewed carefully, it has been established that there is a predominant, radial diffusion direction at an early stage in the developing brain[64,91].

White matter diseases. The potential of 'plain' dMRI in neurology has been assessed in brain tumour grading[92–94], trauma[95], hypertensive hydrocephalus[96], AIDS[97], ECLAMPSIA[98], LEUKOARAIOSIS[99,100], migraine[101] and diseases of the spinal cord in animals[34,102–104] and humans[105,106]. These clinical studies have been motivated by the high sensitivity of dMRI to microstructural changes in tissues, so that anomalies can be detected before changes appear in more conventional images contrasted by the T1 or T2 relaxation times. In some cases, specific (although often speculative) mechanisms underlying physiopathology (oedema, WALLERIAN DEGENERATION, neurotoxicity, swelling and so on) could be proposed, but a clear association between ADC findings and these microstructural tissue alterations remains difficult to demonstrate. Animal models, tissue modelling and computer simulations might help.

In white matter, any change in tissue orientation patterns inside the MRI voxel would probably result in a change in the degree of anisotropy. There is a growing body of literature that supports this assumption. Many clinical studies carried out on patients with white matter diseases have shown the exquisite sensitivity of DTI to abnormalities at an early stage, and the capacity for DTI to characterize these changes in terms of the integrity of white matter fibres. In white matter, dMRI has already shown its potential for use in diseases such as multiple sclerosis[107]. However, DTI offers even more, through the separation of mean diffusivity indices (such as the trace of the diffusion tensor, which reflects overall water content) and anisotropy indices (which reflect myelin fibre integrity). Examples include multiple sclerosis[108–111], leukoencephalopathies[112,113], Wallerian degeneration, human immunodeficiency virus-1 infection[114], Alzheimer's disease[115,116] and CADASIL (cerebral autosomal dominant anteriopathy with subcortical infarcts and leukoencephalopathy)[117] (see REF. 118 for a review).

dMRI could also unravel more subtle, functional disorders that do not necessarily translate into anatomical anomalies. For instance, anisotropy measurements might highlight subtle anomalies in the organization of white matter tracks that are not evident with plain, anatomical MRI. The potential is enormous for patients with functional symptoms linked to disconnectivity; for instance, in patients with psychiatric disorders (see REF. 119 for a review). Links between cognitive impairments and abnormal connectivity in white matter based on DTI MRI data have also been reported in frontal regions of patients with schizophrenia[120,121], in the corpus callosum and the centrum semiovale in patients with chronic alcoholism[122], in left temporoparietal regions in adults with dyslexia[123], and in specific disconnection syndromes[124].

Brain development. Over the course of life, white matter matures and declines. The effects of ageing on white matter ordering can now be studied[122,125], but DTI

can also be used to monitor the myelination process in fetuses, babies and during childhood[126]. DTI has potential importance for the paediatric population[127]. It has been shown that the degree of diffusion anisotropy in white matter increases during the myelination process[64,66,128], so that dMRI could be used to assess brain maturation in children[129], newborns or premature babies[64,130], as well as to characterize white matter disorders in children[131]. Brain development has recently received much research attention. Advances in neuroimaging have contributed to this expansion, as data can now be obtained non-invasively in newborns or even before birth. Of particular interest is the observation made using DTI that water diffusion in white matter in the brain changes markedly during development, in terms of both average and anisotropic diffusion. In grey matter, although water diffusion seems isotropic to some extent in the adult brain cortex, there is a short time window when anisotropy occurs. This transient anisotropy effect probably reflects the migration and organization of glial cells and neurons (for example, dendritic architecture of pyramidal cells) in the cortical layers[64,91]. During postnatal development of white matter, the degree of water diffusion anisotropy reflects the myelination process[127], but the effect is small compared with the prenatal stage, during which a large degree of anisotropy is observed even before axons are myelinated[70]. The combined effects of axon packing in the fibre bundles and thickness of the myelin sheath on the degree of anisotropy are yet to be described in detail, but DTI already represents an outstanding tool to study brain development in animals and humans. Grey matter migration disorders can also be assessed[132,133] using this technique.

Conclusion

It is important to remember that diffusion imaging is a truly quantitative method that gives direct insight into the voxel-averaged microscopic physical properties of tissues (for example, cell size and shape, geometric packing, and so on) through observation of the random translational molecular movement. Many theoretical and experimental analyses on the effects of restriction, membrane permeability, hindrance and tissue inhomogeneity have underlined the care that must be taken to properly interpret DTI data and to infer accurate information on the microstructure and microdynamics of biological systems. With these difficulties in mind, at its current stage of development, DTI is the only approach available to track white matter fibres non-invasively in the human brain and to address anatomical connectivity. In combination with fMRI, which outlines activated cortical networks and might provide clues to functional connectivity, DTI should have a tremendous impact on brain function studies, from animal models to human neuroscience.

DTI is increasingly being used to identify subtle connectivity anomalies in various dysfunctions, such as brain tumours, dyslexia, multiple sclerosis and schizophrenia, and is becoming part of many routine clinical protocols. Powerful improvements to DTI, such as the possibility of looking at the diffusion of

ECLAMPSIA
Seizures that occur in pregnant or puerperal women in association with hypertension, proteinuria or oedema.

LEUKOARAIOSIS
A periventricular increase in the intensity of white matter that is revealed by magnetic resonance imaging. Leukoaraiosis is frequently found in elderly people, and is commonly unrelated to any clinical manifestations.

WALLERIAN DEGENERATION
A form of degeneration occurring in nerve fibres as a result of their division. Named after A. V. Waller, who published an account of it in 1850.

metabolites through magnetic resonance spectroscopy, or the use of 'q-space' imaging, will doubtless take diffusion imaging to new heights. For example, one might observe actual molecular displacement distributions through q-space measurements[134,135]; using this technique, dMRI data can be used to provide a more direct view of the displacements of water molecules[136], which reflect tissue microarchitecture. With the advent of very-high-field magnets (above 10 T), which will push the spatial and temporal limits of MRI, one might expect to break new ground in the already flourishing field of diffusion imaging.

1. Einstein, A. *Investigations on the Theory of Brownian Motion* (eds Furthe, R. & Cowper, A. D.) (Dover, New York, 1956).
2. Le Bihan, D. & Breton, E. Imagerie de diffusion *in vivo* par résonance magnétique nucléaire. *C. R. Acad. Sci. (Paris)* **301**, 1109–1112 (1985).
3. Merboldt, K. D., Hanicke, W. & Frahm, J. Self-diffusion NMR imaging using stimulated echoes. *J. Magn. Reson.* **64**, 479–486 (1985).
4. Taylor, D. G. & Bushell, M. C. The spatial mapping of translational diffusion coefficients by the NMR imaging technique. *Phys. Med. Biol.* **30**, 345–349 (1985).
5. Le Bihan, D. Molecular diffusion, tissue microdynamics and microstructure. *NMR Biomed.* **8**, 375–386 (1995).
6. Lauterbur, P. C. Image formation by induced local interactions: examples employing nuclear magnetic resonance. *Nature* **242**, 190–191 (1973).
7. Kumar, A., Welti, D. & Ernst, R. NMR Fourier zeugmatography. *J. Magn. Reson.* **18**, 69–83 (1975).
8. Stejskal, E. O. & Tanner, J. E. Spin diffusion measurements: spin echoes in the presence of a time-dependent field gradient. *J. Chem. Phys.* **42**, 288–292 (1965).
9. Le Bihan, D. in *Diffusion and Perfusion Magnetic Resonance Imaging. Applications to Functional MRI* (ed. Le Bihan, D.) (Raven, New York, 1995).
10. Tanner, J. E. Self-diffusion of water in frog muscle. *Biophys. J.* **28**, 107–116 (1979).
11. Tanner, J. E. Transient diffusion in a system partitioned by permeable barriers. Application to NMR measurements with a pulsed field gradient. *J. Chem. Phys.* **69**, 1748–1754 (1978).
12. Cooper, R. L., Chang, D. B., Young, A. C., Martin, J. & Ancker-Johnson, B. Restricted diffusion in biophysical systems. *Biophys. J.* **14**, 161–177 (1974).
13. Le Bihan, D. *et al.* MR imaging of intravoxel incoherent motions: application to diffusion and perfusion in neurologic disorders. *Radiology* **161**, 401–407 (1986).
14. Bougeault, P. & Geleyn, J. F. Some problems of closure assumption and scale dependency in the parameterization of moist deep convection for numerical weather prediction. *Meteorol. Atmos. Phys.* **40**, 123–135 (1988).
15. Callaghan, P. T. *Principles of Nuclear Magnetic Resonance Microscopy* (Oxford Univ. Press, Oxford, 1991).
16. Anderson, A. W. & Gore, J. C. Analysis and correction of motion artifacts in diffusion weighted imaging. *Magn. Reson. Med.* **32**, 379–387 (1994).
17. Baird, A. E. & Warach, S. Magnetic resonance imaging of acute stroke. *J. Cereb. Blood Flow Metab.* **18**, 583–609 (1998).
18. Chien, D. *et al.* MR diffusion imaging of cerebral infarction in humans. *Am. J. Neuroradiol.* **13**, 1097–1102 (1992).
19. Moseley, M. E. *et al.* Diffusion-weighted MR imaging of acute stroke: correlation with T2-weighted and magnetic susceptibility-enhanced MR imaging in cats. *Am. J. Neuroradiol.* **11**, 423–429 (1990).
20. Mintorovitch, J. *et al.* Comparison of diffusion- and T2-weighted MRI for the early detection of cerebral ischemia and reperfusion in rats. *Magn. Reson. Med.* **18**, 39–50 (1991).
21. Hossmann, K. A. & Hoehn Berlage, M. Diffusion and perfusion MR imaging of cerebral ischemia. *Cerebrovasc. Brain Metab. Rev.* **7**, 187–217 (1995).
22. Sotak, C. H. The role of diffusion tensor imaging in the evaluation of ischemic brain injury — a review. *NMR Biomed.* **15**, 561–569 (2002).
23. Warach, S., Chien, D., Li, W., Ronthal, M. & Edelman, R. R. Fast magnetic resonance diffusion-weighted imaging of acute human stroke. *Neurology* **42**, 1717–1723 (1992).
24. Sorensen, A. G. *et al.* Hyperacute stroke: evaluation with combined multisection diffusion-weighted and hemodynamically weighted echo-planar MR imaging. *Radiology* **199**, 391–401 (1996).
25. Sorensen, A. G. *et al.* Hyperacute stroke: simultaneous measurement of relative cerebral blood volume, relative cerebral blood flow, and mean tissue transit time. *Radiology* **210**, 519–527 (1999).
26. Knight, R. A. *et al.* Temporal evolution of ischemic damage in rat brain measured by proton nuclear magnetic resonance imaging. *Stroke* **22**, 802–808 (1991).
27. Norris, D. G., Niendorf, T. & Leibfritz, D. Healthly and infarcted brain tissues studied at short diffusion times: the origins of apparent restriction and the reduction in apparent diffusion coefficient. *NMR Biomed.* **7**, 304–310 (1994).
28. Rohl, L. *et al.* Viability thresholds of ischemic penumbra of hyperacute stroke defined by perfusion-weighted MRI and apparent diffusion coefficient. *Stroke* **32**, 1140–1146 (2001).
29. Warach, S., Boska, M. & Welch, K. M. A. Pitfalls and potential of clinical diffusion-weighted MR imaging in acute stroke. *Stroke* **28**, 481–482 (1997).
30. Warach, S., Dashe, J. F. & Edelman, R. R. Clinical outcome in ischemic stroke predicted by early diffusion-weighted and perfusion magnetic resonance imaging: a preliminary analysis. *J. Cereb. Blood Flow Metab.* **16**, 53–59 (1996).
31. Lovblad, K. O. *et al.* Ischemic lesion volumes in acute stroke by diffusion-weighted magnetic resonance imaging correlate with clinical outcome. *Ann. Neurol.* **42**, 164–170 (1997).
32. Gonzalez, R. G. *et al.* Diffusion-weighted MR imaging: diagnostic accuracy in patients imaged within 6 hours of stroke symptom onset. *Radiology* **210**, 155–162 (1999).
33. Warach, S., Boska, M. & Welch, K. M. Pitfalls and potential of clinical diffusion-weighted MR imaging in acute stroke. *Stroke* **28**, 481–482 (1997).
34. Dreher, W. *et al.* Temporal and regional changes during focal ischemia in rat brain studied by proton spectroscopic imaging and quantitative diffusion NMR imaging. *Magn. Reson. Med.* **39**, 878–888 (1998).
35. Basser, P. J. & Jones, D. K. Diffusion-tensor MRI: theory, experimental design and data analysis — a technical review. *NMR Biomed.* **15**, 456–467 (2002).
36. Bammer, R. *et al.* Diffusion tensor imaging using single-shot SENSE–EPI. *Magn. Reson. Med.* **48**, 128–136 (2002).
37. Bammer, R. *et al.* Improved diffusion-weighted single-shot echo-planar imaging (EPI) in stroke using sensitivity encoding (SENSE). *Magn. Reson. Med.* **46**, 548–554 (2001).
38. Vavrek, R. M. & MacFall, J. R. in *Diffusion and Perfusion Magnetic Resonance Imaging. Applications to Functional MRI* (ed. Le Bihan, D.) 67–72 (Raven, New York, 1995).
39. Ogawa, S. *et al.* Intrinsic signal changes accompanying sensory stimulation — functional brain mapping with magnetic resonance imaging. *Proc. Natl Acad. Sci. USA* **89**, 5951–5955 (1992).
40. Logothetis, N. K. The neural basis of the blood-oxygen-level-dependent functional magnetic resonance imaging signal. *Phil. Trans. R. Soc. Lond. B* **357**, 1003–1037 (2002).
41. Zhong, J., Petroff, O. A. C., Prichard, J. W. & Gore, J. C. Changes in water diffusion and relaxation properties of rat cerebrum during status epilepticus. *Magn. Reson. Med.* **30**, 241–246 (1993).
42. Darquie, A., Poline, J. B., Poupon, C., Saint Jalmes, H. & Le Bihan, D. Transient decrease in water diffusion observed in human occipital cortex during visual stimulation. *Proc. Natl Acad. Sci. USA* **98**, 9391–9395 (2001).
43. Cohen, L. B. Changes in neuron structure during action potential propagation and synaptic transmission. *Physiol. Rev.* **53**, 373–418 (1973).
44. Andrew, R. D. & MacVicar, B. A. Imaging cell volume changes and neuronal excitation in the hippocampal slice. *Neuroscience* **62**, 371–383 (1994).
45. Ransom, B. R., Yamate, C. L. & Connors, B. W. Activity-dependent shrinkage of extracellular space in rat optic nerve: a developmental study. *J. Neurosci.* **5**, 532–535 (1985).
46. Svoboda, J. & Sykova, E. Extracellular space volume changes in the rat spinal cord produced by nerve stimulation and peripheral injury. *Brain Res.* **560**, 216–224 (1991).
47. Crick, F. Do dentritic spines twitch? *Trends Neurosci.* **5**, 44–47 (1982).
48. Halpain, S. Actin and the agile spine: how and why do dendritic spines dance? *Trends Neurosci.* **23**, 141–146 (2000).
49. Cleveland, G. G., Chang, D. C., Hazelwood, C. F. & Rorschach, H. E. Nuclear magnetic resonance measurement of skeletal muscle. Anisotropy of the diffusion coefficient of the intracellular water. *Biophys. J.* **16**, 1043–1053 (1976).
50. Hansen, J. R. Pulsed NMR study of water mobility in muscle and brain tissue. *Biochim. Biophys. Acta* **230**, 482–486 (1971).
51. Moseley, M. E., Cohen, Y. & Mintorovitch, J. Early detection of regional cerebral ischemic injury in cats: evaluation of diffusion and T2-weighted MRI and spectroscopy. *Magn. Reson. Med.* **14**, 330–346 (1990).
52. Chenevert, T. L., Brunberg, J. A. & Pipe, J. G. Anisotropic diffusion within human white matter: demonstration with NMR techniques *in vivo*. *Radiology* **177**, 401–405 (1990).
53. Beaulieu, C. The basis of anisotropic water diffusion in the nervous system — a technical review. *NMR Biomed.* **15**, 435–455 (2002).
54. Douek, P., Turner, R., Pekar, J., Patronas, N. J. & Le Bihan, D. MR color mapping of myelin fiber orientation. *J. Comput. Assist. Tomogr.* **15**, 923–929 (1991).
55. Basser, P. J., Mattiello, J. & Le Bihan, D. MR diffusion tensor spectroscopy and imaging. *Biophys. J.* **66**, 259–267 (1994).
56. Basser, P. J., Mattiello, J. & Le Bihan, D. Estimation of the effective self-diffusion tensor from the NMR spin echo. *J. Magn. Reson.* **103**, 247–254 (1994).
57. Le Bihan, D. & van Zijl, P. From the diffusion coefficient to the diffusion tensor. *NMR Biomed.* **15**, 431–434 (2002).
58. Basser, P. J. in *Imaging Brain Structure and Function* (eds Lester, D. S., Felder, C. C. & Lewis, E. N.) 123–138 (New York Academy of Sciences, New York, 1997).
59. Basser, P. J. & Pierpaoli, C. Microstructural and physiological features of tissues elucidated by quantitative-diffusion-tensor MRI. *J. Magn. Reson.* **111**, 209–219 (1996).
60. Pajevic, S. & Pierpaoli, C. Color schemes to represent the orientation of anisotropic tissues from diffusion tensor data: application to white matter fiber tract mapping in the human brain. *Magn. Reson. Med.* **42**, 526–540 (1999).
61. Moseley, M. E., Cohen, Y. & Kucharczyk, J. Diffusion-weighted MR imaging of anisotropic water diffusion in cat central nervous system. *Radiology* **176**, 439–446 (1990).
62. Turner, R. *et al.* Echo-planar imaging of intravoxel incoherent motions. *Radiology* **177**, 407–414 (1990).
63. Rutherford, M. A. *et al.* MR imaging of anisotropically restricted diffusion in the brain of neonates and infants. *J. Comput. Assist. Tomogr.* **15**, 188–198 (1991).
64. Neil, J. J. *et al.* Normal brain in human newborns: apparent diffusion coefficient and diffusion anisotropy measured by using diffusion tensor MR imaging. *Radiology* **209**, 57–66 (1998).
65. Toft, P. B., Leth, H., Peitersen, B., Lou, H. C. & Thomsen, C. The apparent diffusion coefficient of water in gray and white matter of the infant brain. *J. Comput. Assist. Tomogr.* **20**, 1006–1011 (1996).
66. Baratti, C., Barnett, A. S. & Pierpaoli, C. Comparative MR imaging study of brain maturation in kittens with T1, T2, and the trace of the diffusion tensor. *Radiology* **210**, 133–142 (1999).
67. Vorisek, I. & Sykova, E. Evolution of anisotropic diffusion in the developing rat corpus callosum. *J. Neurophysiol.* **78**, 912–919 (1997).
68. Prayer, D. *et al.* Diffusion-weighted MRI of myelination in the rat brain following treatment with gonadal hormones. *Neuroradiology* **39**, 320–325 (1997).
69. Takeda, K. *et al.* MR assessment of normal brain development in neonates and infants: Comparative study of T1- and diffusion-weighted images. *J. Comput. Assist. Tomogr.* **21**, 1–7 (1997).
70. Beaulieu, C., Fenrich, F. R. & Allen, P. S. Multicomponent water proton transverse relaxation and T2-discriminated water diffusion in myelinated and nonmyelinated nerve. *Magn. Reson. Imaging* **16**, 1201–1210 (1998).
71. Le Bihan, D., Turner, R. & Douek, P. Is water diffusion restricted in human brain white matter? An echo-planar NMR imaging study. *Neuroreport* **4**, 887–890 (1993).
72. Moonen, C. T. W. *et al.* Restricted and anisotropic displacement of water in healthy cat brain and in stroke studied by NMR diffusion imaging. *Magn. Reson. Med.* **19**, 327–332 (1991).
73. Clark, C. A. & Le Bihan, D. Water diffusion compartmentation and anisotropy at high b values in the human brain. *Magn. Reson. Med.* **44**, 852–859 (2000).
74. Hajnal, J. V., Doran, M. & Hall, A. S. MR imaging of anisotropically restricted diffusion of water in the nervous system: technical, anatomic, and pathological considerations. *J. Comput. Assist. Tomogr.* **15**, 1–18 (1991).
75. Sakuma, H. *et al.* Adult and neonatal human brain: diffusional anisotropy and myelination with diffusion-weighted MR imaging. *Radiology* **180**, 229–233 (1991).
76. Assaf, Y. & Cohen, Y. Detection of different water populations in brain tissue using ²H single- and double-quantum-filtered diffusion NMR spectroscopy. *J. Magn. Reson.* **112**, 151–159 (1996).

77. Silva, M. D. *et al.* Deconvolution of compartmental water diffusion coefficients in yeast-cell suspensions using combined T1 and diffusion measurements. *J. Magn. Reson.* **156**, 52–63 (2002).

78. Sukstanskii, A. L. & Yablonskiy, D. A. Effects of restricted diffusion on MR signal formation. *J. Magn. Reson.* **157**, 92–105 (2002).

79. Mori, S. & van Zijl, P. C. M. Fiber tracking: principles and strategies — a technical review. *NMR Biomed.* **15**, 468–480 (2002).

80. Mori, S., Crain, B. J., Chacko, V. P. & van Zijl, P. C. M. Three-dimensional tracking of axonal projections in the brain by magnetic resonance imaging. *Ann. Neurol.* **45**, 265–269 (1999).

81. Conturo, T. E. *et al.* Tracking neuronal fiber pathways in the living human brain. *Proc. Natl Acad. Sci. USA* **96**, 10422–10427 (1999).

82. Poupon, C. *et al.* Regularization of diffusion-based direction maps for the tracking of brain white matter fascicles. *Neuroimage* **12**, 184–195 (2000).

83. Mangin, J. F. *et al.* A framework based on spin glass models for the inference of anatomical connectivity from diffusion-weighted MR data — a technical review. *NMR Biomed.* **15**, 481–492 (2002).

84. Koch, M. A., Norris, D. G. & Hund-Georgiadis, M. An investigation of functional and anatomical connectivity using magnetic resonance imaging. *Neuroimage* **16**, 241–250 (2002).

85. Lin, C. P., Tseng, W. Y. I., Cheng, H. C. & Chen, J. H. Validation of diffusion tensor magnetic resonance axonal fiber imaging with registered manganese-enhanced optic tracts. *Neuroimage* **14**, 1035–1047 (2001).

86. Ananth, H. *et al.* Cortical and subcortical gray matter abnormalities in schizophrenia determined through structural magnetic resonance imaging with optimized volumetric voxel-based morphometry. *Am. J. Psychiatry* **159**, 1497–1505 (2002).

87. Rugg-Gunn, F. J., Eriksson, S. H., Symms, M. R., Barker, G. J. & Duncan, J. S. Diffusion tensor imaging of cryptogenic and acquired partial epilepsies. *Brain* **124**, 627–636 (2001).

88. Frank, L. R. Anisotropy in high angular resolution diffusion-weighted MRI. *Magn. Reson. Med.* **45**, 935–939 (2001).

89. Wiegell, M. R., Larsson, H. B. W. & Wedeen, V. J. Fiber crossing in human brain depicted with diffusion tensor MR imaging. *Radiology* **217**, 897–903 (2000).

90. Tuch, D. S. *et al.* High angular resolution diffusion imaging reveals intravoxel white matter fiber heterogeneity. *Magn. Reson. Med.* **48**, 577–582 (2002).

91. Mori, S. *et al.* Diffusion tensor imaging of the developing mouse brain. *Magn. Reson. Med.* **46**, 18–23 (2001).

92. Le Bihan, D. *et al.* Diffusion and perfusion magnetic resonance imaging in brain tumors. *Top. Magn. Reson. Imaging* **5**, 25–31 (1993).

93. Ikezaki, K. *et al.* Apparent diffusion coefficient (ADC) and magnetization transfer contrast (MTC) mapping of experimental brain tumor. *Acta Neurochir. Suppl. (Wien)* **70**, 170–172 (1997).

94. Krabbe, K. *et al.* MR diffusion imaging of human intracranial tumours. *Neuroradiology* **39**, 483–489 (1997).

95. Barzo, P., Marmarou, A., Fatouros, P., Hayasaki, K. & Corwin, F. Contribution of vasogenic and cellular edema to traumatic brain swelling measured by diffusion-weighted imaging. *J. Neurosurg.* **87**, 900–907 (1997).

96. Schwartz, R. B., Mulkern, R. V., Gudbjartsson, H. & Jolesz, F. Diffusion-weighted MR imaging in hypertensive encephalopathy: clues to pathogenesis. *Am. J. Neuroradiol.* **19**, 859–862 (1998).

97. Chang, L. & Ernst, T. MR spectroscopy and diffusion-weighted MR imaging in focal brain lesions in AIDS. *Neuroimaging Clin. N. Am.* **7**, 409–426 (1997).

98. Schaefer, P. W., Buonanno, F. S., Gonzalez, R. G. & Schwamm, L. H. Diffusion-weighted imaging discriminates between cytotoxic and vasogenic edema in a patient with eclampsia. *Stroke* **28**, 1082–1085 (1997).

99. Okada, K., Wu, L. H. & Kobayashi, S. Diffusion-weighted MRI in severe leukoaraiosis. *Stroke* **30**, 478–479 (1999).

100. Jones, D. K. *et al.* Characterization of white matter damage in ischemic leukoaraiosis with diffusion tensor MRI. *Stroke* **30**, 393–397 (1999).

101. Chabriat, H. *et al.* Decreased hemispheric water mobility in hemiplegic migraine related to mutation of *CACNA1A* gene. *Neurology* **54**, 510–512 (2000).

102. Gulani, V. *et al.* A multiple echo pulse sequence for diffusion tensor imaging and its application in excised rat spinal cords. *Magn. Reson. Med.* **38**, 868–873 (1997).

103. Ford, J. C., Hackney, D. B., Lavi, E., Phillips, M. & Patel, U. Dependence of apparent diffusion coefficients on axonal spacing, membrane permeability, and diffusion time in spinal cord white matter. *J. Magn. Reson. Imaging* **8**, 775–782 (1998).

104. Inglis, B. A., Yang, L., Wirth, E. D. III, Plant, D. & Mareci, T. H. Diffusion anisotropy in excised normal rat spinal cord measured by NMR microscopy. *Magn. Reson. Imaging* **15**, 441–450 (1997).

105. Clark, C. A., Barker, G. J. & Tofts, P. S. Magnetic resonance diffusion imaging of the human cervical spinal cord *in vivo*. *Magn. Reson. Med.* **41**, 1269–1273 (1999).

106. Ries, M., Jones, R. A., Dousset, V. & Moonen, C. T. W. Diffusion tensor MRI of the spinal cord. *Magn. Reson. Med.* **44**, 884–892 (2000).

107. Ono, J., Harada, K., Mano, T., Sakurai, K. & Okada, S. Differentiation of dys- and demyelination using diffusional anisotropy. *Pediatr. Neurol.* **16**, 63–66 (1997).

108. Werring, D. J., Clark, C. A., Barker, G. J., Thompson, A. J. & Miller, D. H. Diffusion tensor imaging of lesions and normal-appearing white matter in multiple sclerosis. *Neurology* **52**, 1626–1632 (1999).

109. Tievsky, A. L., Ptak, T. & Farkas, J. Investigation of apparent diffusion coefficient and diffusion tensor anisotropy in acute and chronic multiple sclerosis lesions. *Am. J. Neuroradiol.* **20**, 1491–1499 (1999).

110. Iwasawa, T. *et al.* Diffusion-weighted imaging of the human optic nerve: a new approach to evaluate optic neuritis in multiple sclerosis. *Magn. Reson. Med.* **38**, 484–491 (1997).

111. Horsfield, M. A., Larsson, H. B., Jones, D. K. & Gass, A. Diffusion magnetic resonance imaging in multiple sclerosis. *J. Neurol. Neurosurg. Psychiatry* **64** (Suppl. 1), S80–S84 (1998).

112. Ay, H. *et al.* Posterior leukoencephalopathy without severe hypertension: utility of diffusion-weighted MRI. *Neurology* **51**, 1369–1376 (1998).

113. Eichler, F. S. *et al.* Proton MR spectroscopic and diffusion tensor brain MR imaging in X-linked adrenoleukodystrophy: initial experience. *Radiology* **225**, 245–252 (2002).

114. Filippi, C. G., Ulug, A. M., Ryan, E., Ferrando, S. J. & van Gorp, W. Diffusion tensor imaging of patients with HIV and normal-appearing white matter on MR images of the brain. *Am. J. Neuroradiol.* **22**, 277–283 (2001).

115. Hanyu, H. *et al.* Increased water diffusion in cerebral white matter in Alzheimer's disease. *Gerontology* **43**, 343–351 (1997).

116. Hanyu, H. *et al.* Diffusion-weighted MR imaging of the hippocampus and temporal white matter in Alzheimer's disease. *J. Neurol. Sci.* **156**, 195–200 (1998).

117. Chabriat, H. *et al.* Clinical severity in CADASIL related to ultrastructural damage in white matter — *in vivo* study with diffusion tensor MRI. *Stroke* **30**, 2637–2643 (1999).

118. Horsfield, M. A. & Jones, D. K. Applications of diffusion-weighted and diffusion tensor MRI to white matter diseases — a review. *NMR Biomed.* **15**, 570–577 (2002).

119. Lim, K. O. & Helpern, J. A. Neuropsychiatric applications of DTI — a review. *NMR Biomed.* **15**, 587–593 (2002).

120. Buchsbaum, M. S. *et al.* MRI white matter diffusion anisotropy and PET metabolic rate in schizophrenia. *Neuroreport* **9**, 425–430 (1998).

121. Lim, K. O. *et al.* Compromised white matter tract integrity in schizophrenia inferred from diffusion tensor imaging. *Arch. Gen. Psychiatry* **56**, 367–374 (1999).

122. Pfefferbaum, A. *et al. In vivo* detection and functional correlates of white matter microstructural disruption in chronic alcoholism. *Alcohol Clin. Exp. Res.* **24**, 1214–1221 (2000).

123. Klingberg, T. *et al.* Microstructure of temporo-parietal white matter as a basis for reading ability: evidence from diffusion tensor magnetic resonance imaging. *Neuron* **25**, 493–500 (2000).

124. Molko, N. *et al.* Visualizing the neural bases of a disconnection syndrome with diffusion tensor imaging. *J. Cogn. Neurosci.* **14**, 629–636 (2002).

125. Moseley, M. Diffusion tensor imaging and aging — a review. *NMR Biomed.* **15**, 553–560 (2002).

126. Schmithorst, V. J., Wilke, M., Dardzinski, B. J. & Holland, S. K. Correlation of white matter diffusivity and anisotropy with age during childhood and adolescence: a cross-sectional diffusion-tensor MR imaging study. *Radiology* **222**, 212–218 (2002).

127. Neil, J., Miller, J., Mukherjee, P. & Huppi, P. S. Diffusion tensor imaging of normal and injured developing human brain — a technical review. *NMR Biomed.* **15**, 543–552 (2002).

128. Takahashi, M., Ono, J., Harada, K., Maeda, M. & Hackney, D. B. Diffusional anisotropy in cranial nerves with maturation: quantitative evaluation with diffusion MR imaging in rats. *Radiology* **216**, 881–885 (2000).

129. Zimmerman, R. A. *et al.* Advances in pediatric neuroimaging. *Brain Dev.* **20**, 275–289 (1998).

130. Huppi, P. S. *et al.* Microstructural development of human newborn cerebral white matter assessed *in vivo* by diffusion tensor magnetic resonance imaging. *Pediatr. Res.* **44**, 584–590 (1998).

131. Engelbrecht, V., Scherer, A., Rassek, M., Witsack, H. J. & Modder, U. Diffusion-weighted MR imaging in the brain in children: findings in the normal brain and in the brain with white matter diseases. *Radiology* **222**, 410–418 (2002).

132. Eriksson, S. H. *et al.* Exploring white matter tracts in band heterotopia using diffusion tractography. *Ann. Neurol.* **52**, 327–334 (2002).

133. Eriksson, S. H., Rugg-Gunn, F. J., Symms, M. R., Barker, G. J. & Duncan, J. S. Diffusion tensor imaging in patients with epilepsy and malformations of cortical development. *Brain* **124**, 617–626 (2001).

134. Assaf, Y. & Cohen, Y. *In vivo* and *in vitro* bi-exponential diffusion of *N*-acetyl aspartate (NAA) in rat brain: a potential structural probe? *NMR Biomed.* **11**, 67–74 (1998).

135. Cohen, Y. & Assaf, Y. High b-value q-space analyzed diffusion-weighted MRS and MRI in neuronal tissues — a technical review. *NMR Biomed.* **15**, 516–542 (2002).

136. Callaghan, P. T. NMR imaging, NMR diffraction and applications of pulsed gradient spin echoes in porous media. *Magn. Reson. Imaging* **14**, 701–709 (1996).

137. Merboldt, K. D., Hörstermann, D., Hänicke, W., Bruhn, H. & Frahm, J. Molecular self-diffusion of intracellular metabolites in rat brain *in vivo* investigated by localized proton NMR diffusion sprectroscopy. *Magn. Reson. Med.* **29**, 125–129 (1993).

138. Posse, S., Cuenod, C. A. & Le Bihan, D. Human brain: proton diffusion MR spectroscopy. *Radiology* **188**, 719–725 (1993).

139. Wick, M., Nagatomo, Y., Prielmeier, F. & Frahm, J. Alteration of intracellular metabolite diffusion in rat brain *in vivo* during ischemia and reperfusion. *Stroke* **26**, 1930–1934 (1995).

140. Sehy, J. V., Ackerman, J. J. H. & Neil, J. J. Apparent diffusion of water, ions, and small molecules in the *Xenopus* oocyte is consistent with Brownian displacement. *Magn. Reson. Med.* **48**, 42–51 (2002).

🌐 Online links

DATABASE
The following terms in this article are linked online to:
OMIM: http://www.ncbi.nlm.nih.gov/Omim/
Alzheimer disease | CADASIL | hydrocephalus | multiple sclerosis
FURTHER INFORMATION
Encyclopedia of Life Sciences: http://www.els.net/
AIDS and the nervous system | dyslexia | human immunodeficiency viruses | migraine | schizophrenia | stroke
Access to this interactive links box is free online.